scientific reports

OPEN

Impacts of environments on school myopia by spatial analysis techniques in Wuhan

Qi Cui[1,2,3], Yishuang Xu[1,3], Fan Li[1,3], Fangyuan Zhou[1], Di Xiao[1], Zhen Chen[1]✉, Xianghong Hua[2]✉ & Dihao Hua[1]✉

The prevalence of myopia in China has increased significantly in recent years, and the age of onset has become younger. Previous studies have indicated that various environmental factors can influence the development of school myopia. However, the environmental impacts on school myopia remains to be investigated. Discoveries in this field may contribute to better urban planning. This study involved 7,610 students (aged 6–12 years, 4084 boys and 3526 girls) from six primary schools in Wuhan, China. We evaluated the associations between school myopia and the environment by analyzing the geographical distribution of myopic children. We utilized the spatial statistical analysis model. The Normalized Difference Vegetation Index (NDVI) risk coefficient for a 5,000-m radius around target schools was 0.379 ($p = 0.008$), while the NDVI risk coefficient for a 100-m radius around target schools was 0.241 ($p = 0.047$). The sports area risk coefficient for a 5,000-m radius around target schools was 0.234 ($p = 0.016$). We found that the specific buffers of NDVI and sports area around schools were associated with the prevalence of school myopia in schools, which worth further research to guide future initiatives on school myopia from an environmental perspective.

Keywords School myopia, Geodetector, NDVI, Sports area, Myopia prevention

Myopia, a refractive disorder, is rapidly becoming a significant public health emergency. By 2050, the incidence of myopia is expected to include five billion people, with 10% diagnosed with high myopia[1]. High myopia is associated with a variety of complications, such as retinal detachment, glaucoma, and posterior staphyloma, which can severely impact quality of life[2–4]. As such, myopia control and prevention, especially in children, are of paramount importance[5].

The research published by the International Myopia Institute highlights time spent studying and time spent outdoors as two major risk factors for school myopia[6]. The increased pressure to study among children in East and Southeast Asia is correlated with a higher amount of near work and a higher risk for myopia[7]. In contrast, time spent engaged in outdoor activities was negatively correlated with myopia rates in children. Time spent outdoors also seemed to be a protective factor against myopia among children who engaged in extensive near-work[8].

Other studies have also demonstrated that myopia is associated with other factors, such as sex, ethnicity, and parental myopia[9]. More recent studies stress the role of environmental factors, like schooling[10–13]. One study has identified air pollution as a likely cause of myopia, suggesting that peripheral hyperopic focus, retinal ischemia, and dopamine pathways may all play a role; however, the precise mechanisms for this correlation remain unclear[12]. Increasingly, green spaces are being identified as a new factor for school myopia[14,15]. For example, children in schools with more green spaces have lower prevalence rates of school myopia[14]. Increasing green spaces around schools may encourage students to engage in outdoor activities[15,16], which indirectly reduces the time spent on near-work[17,18].

While groundbreaking, the methodology in the existing research does leave room for improvements[15]. For example, the existing research only analyzed areas as “urban” and “rural” but did not factor in potential similarities in the geographical features between these spaces[19,20]. A spatial research approach grounded in regional clustering characteristics is likely more suitable and precise. As such, this paper aims to examine the association between school myopia and the environment using geographical methods. We hope to use our findings to guide city planning and school myopia control.

[1]Eye Center, Renmin Hospital of Wuhan University, Wuhan 430060, Hubei, China. [2]School of Geodesy, Wuhan University, Wuhan 430079, Hubei, China. [3]Qi Cui, Yishuang Xu and Fan Li contributed equally to this work. ✉email: hchenzhen@163.com; xhhua@sgg.whu.edu.cn; dihaohuaphd@163.com

The Normalized Difference Vegetation Index (NDVI) is widely used to evaluate green spaces. Its distribution typically varies across different cities because of diverse environmental district planning differences[21]. Previous studies reported that school myopia was negatively correlated with specific NDVI buffers[22,23]. For instance, a high school in Beijing with an NDVI within 500-m radius showed lower rates of myopia among its high school students[22]. A primary school in Guangzhou with a similar NDVI within a 300-m radius demonstrated similar protective effects[23].

Wuhan is a city located in the middle of China. It shows unique environmental characteristics that resemble those seen in northern Beijing and southern Guangzhou. This mix makes it an interesting location for the study of the environment's impact on school myopia. From climate perspective, Beijing and Guangzhou have temperate and tropical monsoon climates, respectively. Comparatively, Wuhan has a subtropical monsoon climate. These climates are associated with different vegetation types and green space morphologies. From a district planning perspective, Wuhan has numerous inner lakes that contribute to uneven green space, road, and school distribution. The same is not observed in Beijing and Guangzhou. Therefore, our study aims to explore the association between primary school myopia and varying NDVI radii buffers in Wuhan using the spatial statistical analysis method. We also utilized the geodetector method to evaluate the interaction between environmental factors, such as NDVI, air quality, sports area, and meteorological data.

Methods

This is a cross-sectional study. The study was approved by the Ethics Committee of Renmin Hospital of Wuhan University (WDRY2020-K234) and followed the tenets of the Declaration of Helsinki. Informed consent was obtained from all the subjects in this study.

Subjects

A total of 7,727 students who were patients of the Eye Center of Renmin Hospital of Wuhan University in 2021 were included in this study. All participants underwent an eye examination, which included visual acuity testing, refraction, and slit-lamp biomicroscopy. Uncorrected visual acuity was assessed for each eye separately using tumbling E Early Treatment Diabetic Retinopathy Study charts at a distance of 4 m in a well-lit indoor area. Non-cycloplegic refraction was performed using a fully automatic computer optometer (RM800; TOPCON, Tokyo, Japan) and subjectively refined by optometrists of the Eye Center. Slit-lamp biomicroscopy was performed by well-trained optometrists to observe the anterior segment. Myopia was diagnosed in all patients with a spherical equivalent and uncorrected visual acuity lower than −0.50D and 1.0, respectively. All examinations were conducted by trained optometrists. Exclusion criteria were as follows: (1) age < 6 or > 12; (2) best corrected visual acuity < 1.0; (3) history of strabismus surgery or intraocular surgery; (4) history of glaucoma, intraocular inflammation, intraocular media opacifications, and retinal diseases; and (5) history of neurodegenerative diseases;

NDVI

NVDI calculations require remote sensing images. As such, the Landsat 8 satellite images were used in this study. To investigate the impact of NDVI on school myopia within different cluster regions, six buffer zones were established with a radius of 50 m, 100 m, 500 m, 1,000 m, 3,000 m, and 5,000 m. The NDVI was calculated as follows:

$$NDVI = \frac{NIR - Red}{NIR + Red} \tag{1}$$

Air quality index

Atmospheric pollution is typically measured by particulate matter (PM), carbon monoxide (CO), nitrogen oxides (NOX), and ozone (O3) concentrations. This study measured the air quality index (AQI) in the summer (April to June) and winter (September to December) seasons to coincide with the school semesters. Data from 23 air quality monitoring stations located within Wuhan were collected. The data was then processed using the kriging interpolation method, which proposes that the value of one point can be derived by the values of its neighboring points. The AQI for six cluster regions was thus estimated with the following formula:

$$\widehat{z_0} = \sum\nolimits_{i=1}^{n} \lambda_i z_i \tag{2}$$

where: $\widehat{z_0}$ is the estimated value at point z_0, and λ_i is the weight coefficient to bring the estimated values closer to the actual values, satisfying:

$$\min_{\lambda_i} Var\left(\widehat{z_0} - z_0\right) \tag{3}$$

Sports area

Sports area within a 5,000-m radius around the cluster regions were identified with the map application programming interface (API), Baidu Map API. Baidu Man API identified all sports facilities in Wuhan, such as football fields, basketball fields, badminton fields, and table tennis fields.

Meteorological data

The meteorological factors that were analyzed in this study included sunshine duration (SSD), precipitation rate (PRE), and mean 2-meter temperature (TEM). The data was obtained with China Meteorological Forcing Dataset Version 3.0, which records information from 699 meteorological stations located throughout China[24].

After being washed and screened, the raw data from the dataset was interpolated by the Kriging method to obtain the meteorological data for the six cluster regions.

Geodetector

A geodetector is a spatial analysis method that can identify spatial variations and its underlying driving forces[25]. Geodetectors have four primary functions: It can (1) explore the geographical factors associated with diseases (risk detection); (2) calculate the explanatory power and rank the hazard of risk factors (factor detection); (3) compare the significance of interactions among different factors (ecological detection); and (4) identify the outcomes of the interactions between different factors (interaction detection). The q value was used to represent the explanatory power of the independent variable on the dependent variable, which ranged between 0 and 1. The formula to calculate the q value is shown as follows:

$$q = 1 - \frac{\sum_{h=1}^{L} N_h \sigma_h^2}{N \sigma^2} \quad (4)$$

where: h is the different layers from 1 to L, N is the number of individuals in all layers, N_h is the number of individuals in layer h, σ^2 is the variance between the layers and σ_h^2 is the variance in layer h.

Statistics

RStudio for Windows (V4.2.3. Boston, MA, USA) was used for data analysis[26]. The χ2 test and analysis of variance with the *post hoc* Bonferroni test were used to assess intergroup differences in categorical and continuous variables, respectively. Our analysis was performed using complete case data without imputation for missing data and dropouts. Two-sided p-values of less than 0.05 were considered statistically significant.

Results

Different data processing methods were selected based on the characteristics of the geographical data. The AQI and meteorological shapefiles were collected and interpolated to the six identified clusters using the Kriging method. The sports area shapefile was collected by Map JavaScript API, and an area calculation algorithm was utilized to calculate the actual sports area. Satellite images were downloaded from Landsat 8 satellites and used to calculate the NDVI after geometric correction, radiometric calibration, and atmospheric correction. These factors were then evaluated for their contribution to school myopia. The processing flowchart is shown below. (Fig. 1)

Demographic data

A total of 7,727 students (4,146 boys and 3,581 girls) underwent eye screening and were included in this study. Five students (2 boys and 3 girls) were excluded because of previous eye surgery, whereas 112 students (60 boys and 52 girls) were excluded because their best corrected visual acuity was lower than 1.0. The remaining 7,610 students (4,084 boys and 3,526 girls) comprised the population of this study. (Table 1).

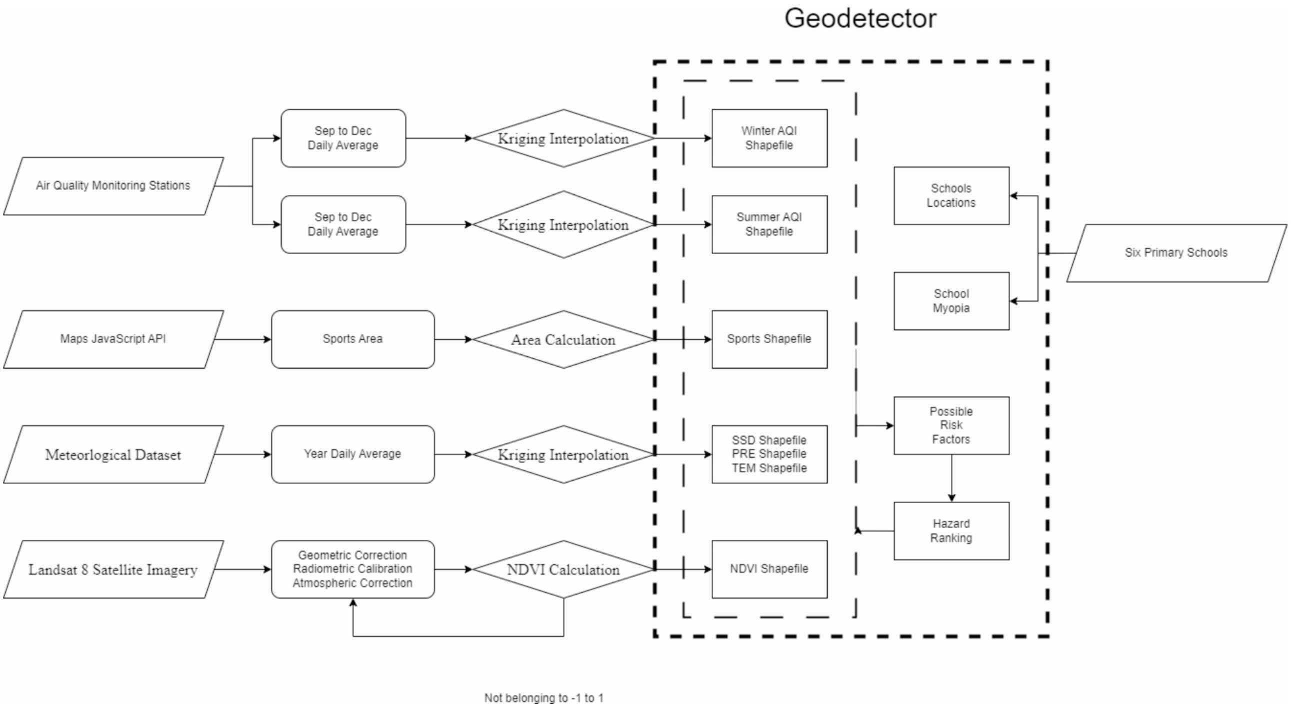

Fig. 1. Geospatial Data Processing Flowchart.

	Boy		Girl		All	
Grade	N	Prevalence	N	Prevalence	N	Prevalence
First Grade	732	2.60%	611	2.29%	1343	2.46%
Second Grade	754	9.28%	634	7.89%	1388	8.65%
Third Grade	705	13.33%	645	16.74%	1350	14.96%
Fourth Grade	725	24.55%	591	27.75%	1316	25.99%
Fifth Grade	599	38.23%	537	44.51%	1136	41.20%
Sixth Grade	569	47.10%	508	53.74%	1077	50.23%
All	4084	21.01%	3526	24.05%	7610	22.42%

Table 1. The prevalence of myopia among students.

	Boy		Girl		All	
Primary school	N	Prevalence	N	Prevalence	N	Prevalence
DF	247	20.65%	254	22.05%	501	21.36%
JH	288	25.69%	234	28.63%	522	27.01%
ZD	747	16.60%	681	21.88%	1428	19.12%
DH	2264	21.51%	1895	23.69%	4159	22.51%
QT	258	24.81%	225	29.78%	483	27.12%
GC	280	20.71%	237	25.32%	517	22.82%
All	4084	21.01%	3526	24.05%	7610	22.42%

Table 2. The prevalence of myopia among primary schools.

The total prevalence of myopia was 22.42%, with 21.01% and 24.05% of boys and girls diagnosed, respectively. The prevalence of myopia increased with grade level. The prevalence of myopia among primary schools is shown in Table 2. Qiaotou Primary School had the highest prevalence of myopia with 27.12%.

The geographical locations of the six primary schools are shown as red points in Fig. 2. These schools were selected because their geographical features reflect the clustering characteristics of the industrial areas, residential areas, and areas of urban-rural integration in Wuhan. (Fig. 2)

NDVI calculation

The *NDVI* map of Wuhan is shown in Fig. 3. Each pixel corresponds to an individual NDVI value, Darker green pixels represent higher NDVI areas, whereas lighter green pixels correspond to lower NDVI areas. Light green pixels typically represented roads or lakes lacking greenery. From the correlation analysis, we observed that there was a significant correlation between the 100-m ($p=0.04$) and 5,000-m ($p=0.03$) NDVI buffer zones and school myopia. An increase in the NDVI value within the 100-m buffer zone around a school was associated with an 18% reduction in the risk of myopia. Comparatively, an increase in the NDVI value within the 5,000-m buffer zone around a school was associated with a 13% reduction in the risk of myopia. (Table 3)

Air quality calculation

The density maps of different pollutants are shown in Fig. 4. Pollutant gases were more prevalent during winter, exhibiting increased concentrations and expanded impact ranges.

Risk and factor detection

Three different models were used to depict the impact of geographical factors on school myopia (Table 4). The q-value represented the explanatory power of the risk factors, with higher q-values indicating a greater risk for school myopia.

Model A was used to describe the explanatory power of the risk factors on school myopia among all students. Among the identified factors, an *NDVI* within a 5,000-m buffer zone, an *NDVI* within a 100-m buffer zone, and the sports area within a 5,000-m buffer zone ranked highest, with explanatory powers of 0.3789, 0.2408, and 0.2335, respectively (all $p<0.05$).

Model B was used to describe the explanatory power among girls. The top three factors included an *NDVI* within a 5,000-m buffer zone, an *NDVI* within a 100-m buffer zone, and the sports area within a 5,000-m buffer zone. These had explanatory powers of 0.4319, 0.2433, and 0.2221, respectively (all $p<0.05$).

Model C was used to describe the explanatory power among boys. As with girls, the top three factors included an NDVI within a 5,000-m buffer zone, an NDVI within a 100-m buffer zone, and the sports area within a 5,000-m buffer zone. The explanatory powers of these factors were 0.32, 0.251, and 0.228, respectively (all $p<0.05$). There was no significant correlation among the other results.

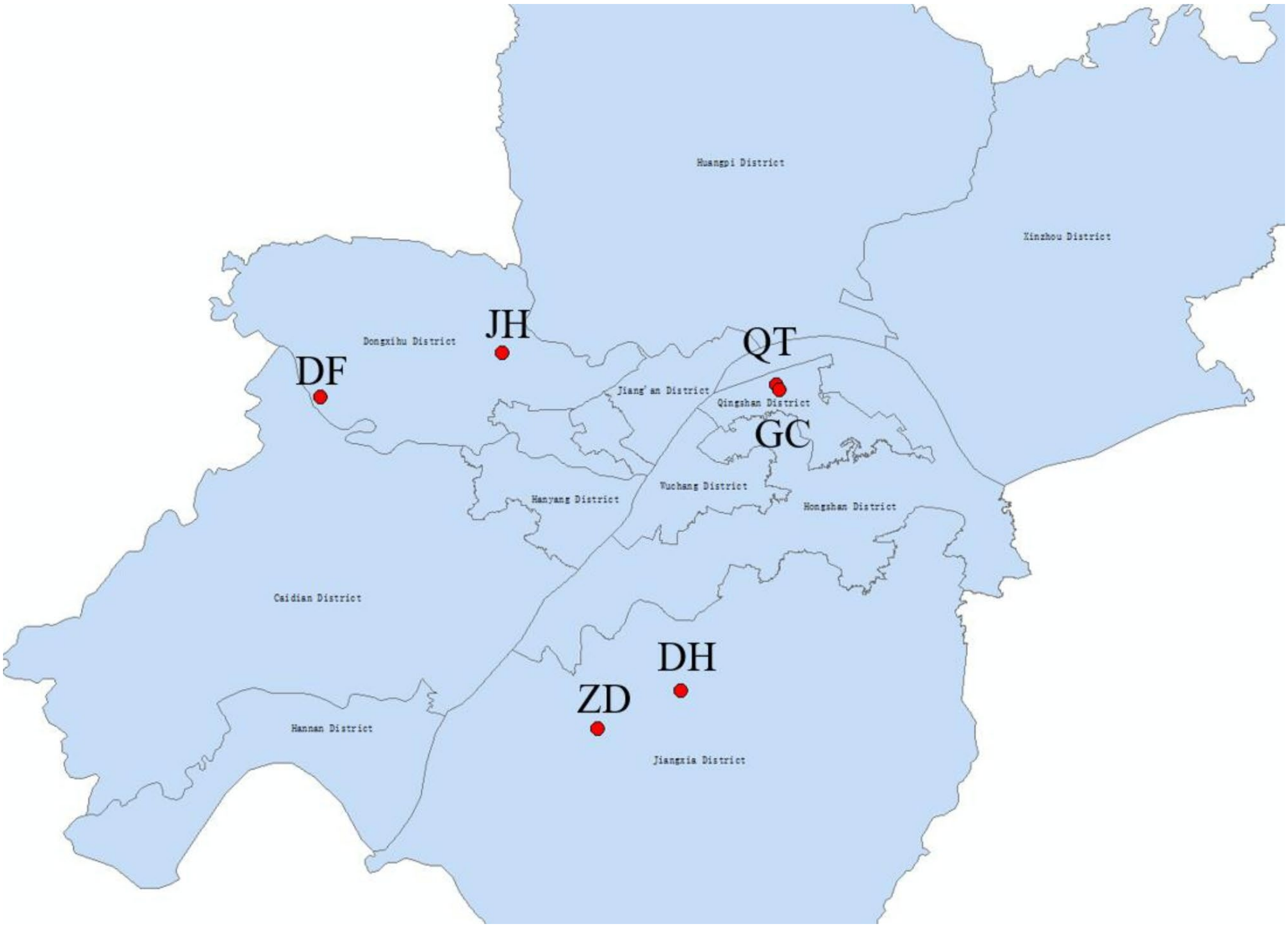

Fig. 2. The geographical locations of the six primary schools.

Interactions detection

Interaction detection identified the independent risk factors associated with school myopia (Table 5), where a different interaction method may be associated with each factor. Two-factor enhancement may be used to explain the mutual enhancement between two factors. Older age strengthened the impact of the NDVI within a 100-m radius. Comparatively, non -linear attenuation may explain the weakening between two factors. Lower summer AQI reduced the impact of the NDVI within a 100-m radius. Single-factor non-linear attenuation can explain the stronger effects of weakness than non-linear attenuation. In Table 5, all factors except for winter AQI exhibited a two-factor enhancement effect that was directly proportional with age. Non-linearly attenuation relationships were also noted between other factor pairs.

Ecological detection

Ecological detection identified a significant difference in the spatial distribution between the two risk factors (Table 6). A significant difference between two factors indicates a dissimilarity between the factors, specifically a dissimilarity in their clustering patterns and distribution features. In contrast, both summer and winter AQIs showed no significant difference with the NDVI in the 100-m buffer zone ($p > 0.05$), which may be due to the cleaning effectiveness of green areas on air quality. In terms of their impact on school myopia, both summer and winter AQI demonstrated no significant difference between each other ($p > 0.05$), indicating that the air pollution during both seasons may be caused by similar factors.

Discussion

Spatial analysis techniques were used to analyze the correlation between various environmental factors and the prevalence of school myopia in six primary schools in Wuhan. In the geodetector model, it was observed that schools with larger green spaces and sports area tended to have a lower prevalence of school myopia. The influence of these factors on school myopia strengthened with age. Although air pollution showed no direct correlation with school myopia, they seemed to diminish the inhibitory effects of green spaces and sports area. By considering various environmental factors and how they interact, individualized district and structural planning strategies can be devised to reduce the prevalence of school myopia.

Numerous studies have supported the association between myopia and green spaces. A study in Shenzhen found that an NDVI increase of 0.1 was associated with a 19.8% decrease in the risk of myopia[13]. A study in

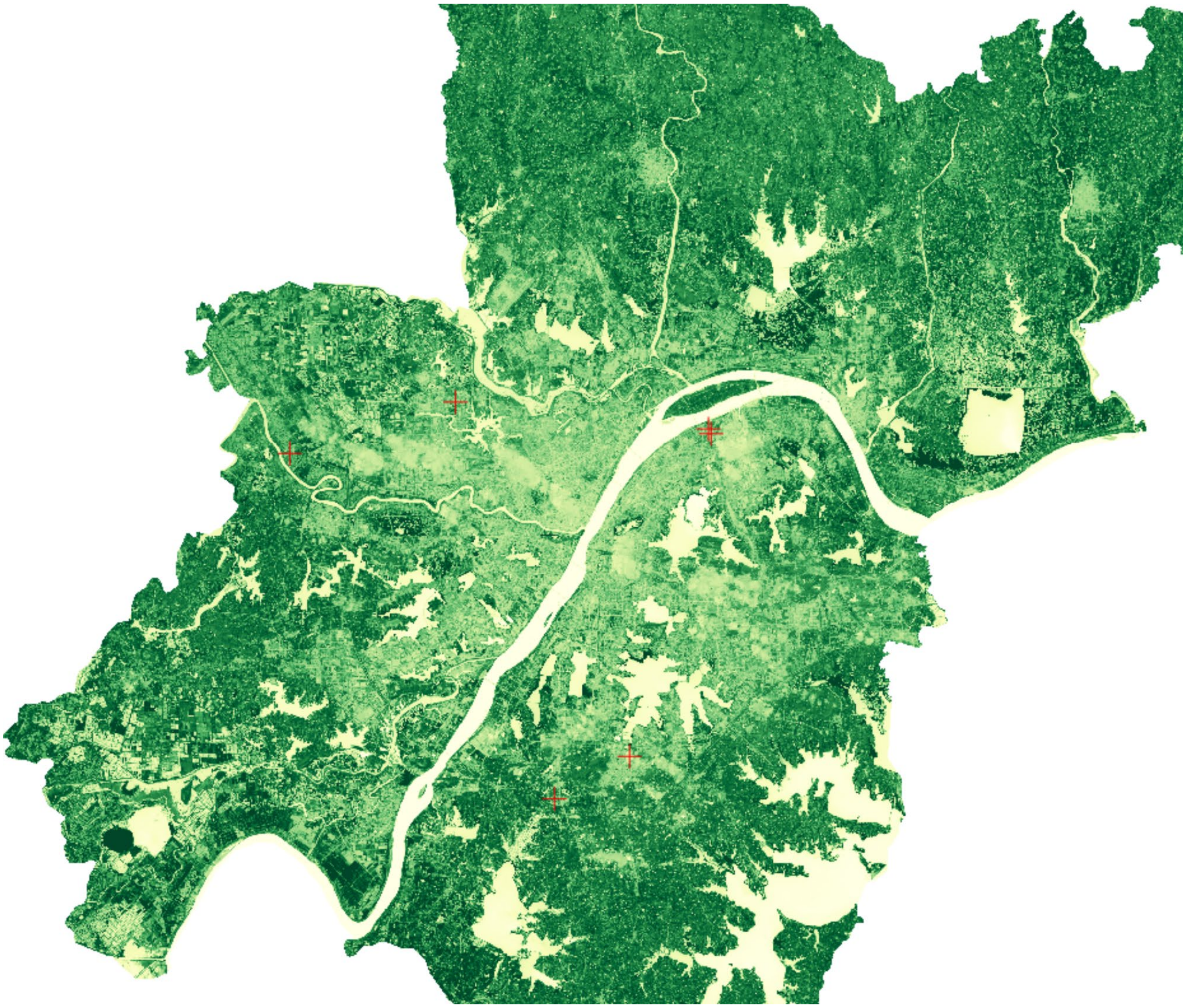

Fig. 3. The NDVI map of Wuhan. The remote sensing images of Wuhan were obtained using Landsat 8 satellite data, accessible via USGS Earth Explorer (https://earthexplorer.usgs.gov/). The Normalized Difference Vegetation Index (NDVI) values, ranging from 0 to 1, were calculated using QGIS software (https://qgis.org/en/site/forusers/download.html, version 3.34.8), to assess vegetation coverage in the region. Data processing and visualization followed standard protocols for remote sensing analysis.

Guangzhou also found that higher NDVI values were associated with lower visual acuity[20]. Similar results have been reported in studies from Australia and Brazil[27,28].

Our study utilized high-resolution satellite data from 2021 to calculate the NDVI within different radii areas around target schools. It was found that enhancing green spaces within 100-m and 5,000-m of these schools effectively reduced the prevalence of school myopia. We speculate that the 100-m radius represented the area within which elementary school students played during school hours. Comparatively, the 5,000-m radius represented the area of their commute or post-school activities. While the reasons were not elucidated, a Beijing study reported that an NDVI within radii of 500-m and 1,000-m around schools effectively delayed the onset of myopia among junior and senior students[22]. From an environmental perspective, Wuhan is an inland city with numerous lakes and hills. These natural bodies of water might widen the distance between schools and residential areas and increase a typical student's commute. In contrast, Beijing follows an evenly distributed rectangular road design, which contributes to shorter commuting distances for students.

Interestingly, previous studies also demonstrated that the NDVI within a 300-m radius of schools in Guangzhou was related to an increased prevalence of school myopia. This varied from the results in Wuhan and Beijing[23]. Although the specific mechanisms by which green spaces affect school myopia remain unclear, several associations have been identified. For instance, green spaces might increase a child's willingness to engage in outdoor activities, which reduces their near-work time[15]. This change in behavior effectively reduces the progression of myopia. Additionally, a previous study found an inverse correlation between spatial frequency and myopia prevalence[29]. Green spaces have higher spatial frequencies than indoor environment[30], which may

Radius	*r*	*p*
50-m	-0.59	0.21
100-m	-0.82	*0.04
500-m	-0.63	0.18
1,000-m	-0.79	0.06
3,000-m	-0.79	0.06
5,000-m	-0.87	*0.03

Table 3. Correlation coefficient and p-value between the NDVI value and the buffer zone radius. * Denotes the statistical significance

protect against school myopia. Research on this topic should be individualized to each city because of intercity differences.

Previous studies also found that time spent in outdoor activities was negatively correlated with school myopia[31,32]. These studies proposed that surrounding sports facilities represented the potential for physical activity. They proposed that increasing the sports area around schools helped control the prevalence of school myopia. Our study utilized sports maps to evaluate the sports area around target schools and contrasts with the traditional survey method[33,34].

This study aimed to determine whether the sports area around a school reduces school myopia. We utilized sports maps to quantify the sports area, which makes our data more reliable. All sports area were equally included in this study, without giving more weight to specific sports. Overall, our data proposed that sports area seemed to be protective against school myopia. Furthermore, larger sports area may be associated with more usage. As such, sports area size may serve as a new indicator of myopia control. Additionally, children who engage in outdoor activities are exposed to more light, which promotes the synthesis and release of retinal dopamine. Retinal dopamine activates dopamine D2 receptors to bind with Gi proteins. This inhibits the activity of adenylate cyclase, which ultimately slows the progression of myopia[35]. More research should be done to examine the relationship between the sports area around schools and school myopia. Insights into this relationship can help guide future initiatives on school myopia from a city-planning perspective.

This study also showed no correlation between air pollution and the prevalence of school myopia. However, our interaction analysis suggested that air pollution may diminish the protective effects of green spaces and sports area on school myopia. For example, when children engage in outdoor activities in polluted green spaces, the exposure to pollutants may directly impact their eyes[36]. Prolonged exposure to PM and NOx can trigger intraocular inflammation[37,38], promote the release of interleukin-6 and transforming growth factor-β, and lead to abnormal axial elongation, which results in myopia[39]. Tangentially, green spaces can also clean the air and reduce pollution levels[40], which may reduce the impact of polluted air on myopia. This relationship may be dependent the cleaning effectiveness of green spaces. In our study, winter air quality had a larger effect on school myopia than summer air quality. This suggests that it may be important to control emissions of factories near schools that release high levels of pollutants in winter. From a district planning perspective, it is necessary to strengthen zoning regulations that keep schools away from industrial areas, which may prove beneficial for controlling school myopia.

There were also other interactions between the identified risk factors. As age increased, the environmental impact on myopia also increased. This implied that individuals of different ages seem to be affected by environmental factors to varying degrees, which may result in differences in growth patterns. As such, different myopia control and prevention strategies should be proposed for different ages and in different regions. For example, senior students may be encouraged to increase their time in green spaces to reduce their risk for myopia. Overall, our study suggested that urban planning and age-based preventive strategies contribute to myopia prevention. Urban planning strategies must be tailored to each geographic location.

Our study has some limitations. First, the participants underwent non-cycloplegic refractive error measurement, which may overestimate the degree of myopia[41,42]. Previous studies identified that the different ages of primary students showed a different prevalence of pseudomyopia, and it was higher in lower-grade students compared to higher-grade students[43]. When comparing refractive errors in different grades, the variance (σ_h) of myopia in formula (4) may be decreased among participants with lower refractive errors and increased among participants with higher refractive errors. Despite this trend, the variance between factors (σ) may remain unchanged, which can inaccurately reduce the explanatory power (q) of risk factors on school myopia. As a result, the relationship of all studied factors on school myopia may be falsely low. Moreover, myopia tended to increase proportionally across all the schools in this study, resulting in a moderate change in the variance(σ) of overall myopia prevalence. This might cause little impact on the explanatory powers of the identified risk factors[15]. Finally, pseudomyopia is an important risk factor for school myopia, and its association with environmental factors deserves future research[44]. Performing large-scale cycloplegic autorefraction is very challenging, and most research on myopia is hampered by this limitation. Recently work has attempted to use artificial intelligence (AI) to replace cycloplegic refraction[45]. An AI-assisted study may be a good endeavor in the future. Second, while our sample size was small, there was no overlap among schools with the same geographic features, including a population located in a region with wide-ranging geographic features, such as industrial areas, residential areas, and areas of urban-rural integration. We also actively engaged in subject recruitment efforts to expand our sample size to ensure more geographic features. Third, this study followed a cross-sectional

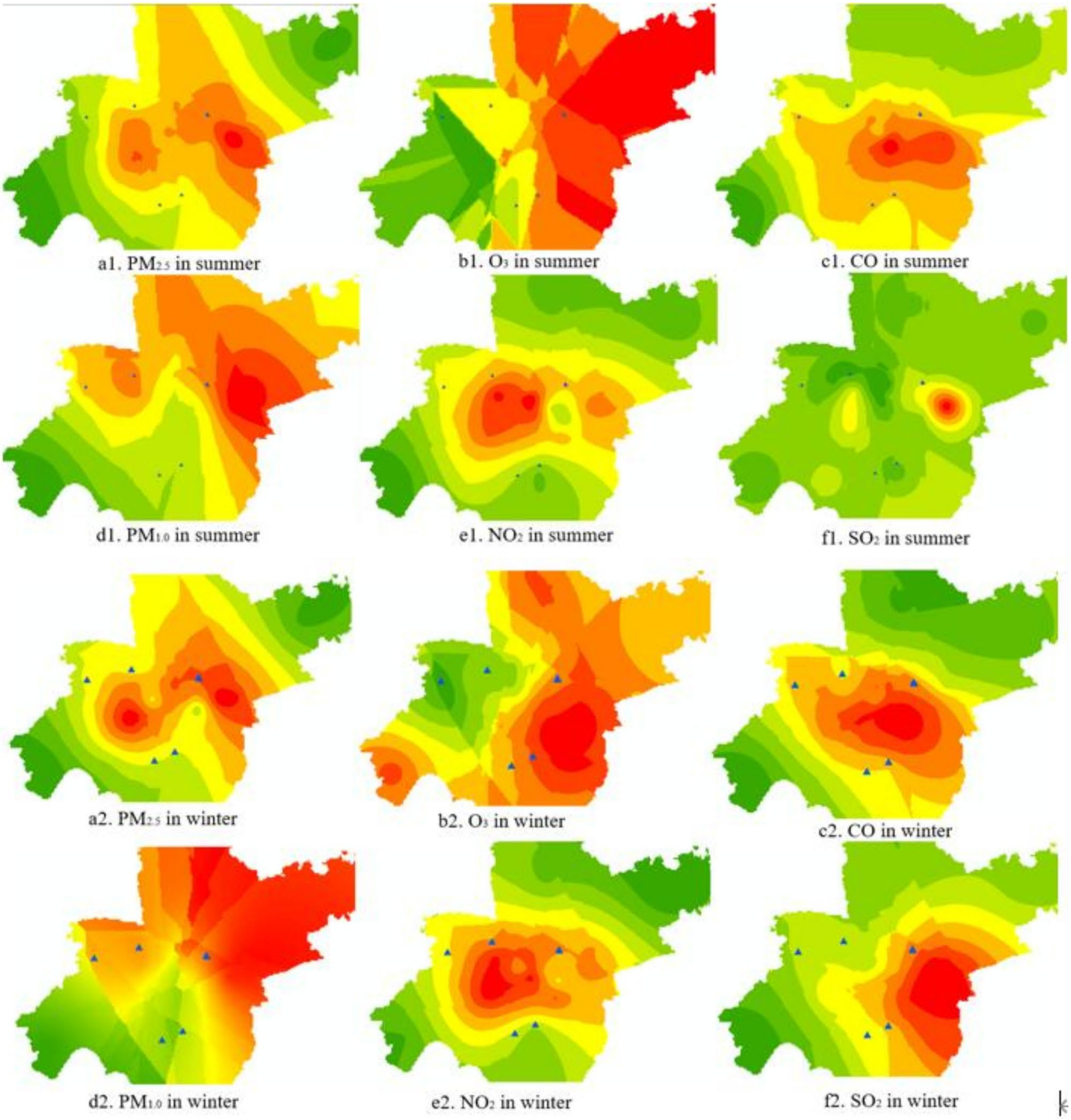

Fig. 4. The air pollutan maps of Wuhan. Labels a1 to f1 represent the distribution of six pollutants in Wuhan in summer, while labels a2 to f2 represent the distribution of six pollutants in winter. The transition from green to red represents an increase in pollution levels. The locations of the six schools are marked with blue triangles on the map. The air quality data for Wuhan were obtained from the Wuhan Natural Resources Bureau website (http://www.whzr.gov.cn/). The pollution maps were created using QGIS software (https://qgis.org/en/site/forusers/download.html, version 3.34.8), to visualize the distribution of air pollutants in the region.

design. The relationship between myopia progression and the environment in this study was only taken at one point in time.

Conclusion

Remote sensing and spatial analysis tools identified a protective effect between green spaces and sports area on the prevalence of school myopia. Relationships between air pollution and myopia were also examined. Modifying these factors may potentially control the prevalence of myopia among school children, which needs further research.

	Model A		Model B		Model C	
Risk factors	q	*p*	q	*p*	q	*p*
NDVI_100m	0.2408	*0.047	0.2433	*0.043	0.2510	*0.049
NDVI_5,000 m	0.3789	*0.008	0.4319	*0.002	0.3200	*0.026
sports area	0.2335	*0.016	0.2221	*0.018	0.2383	*0.015
AQI_winter	0.1317	0.154	0.1158	0.181	0.1559	0.109
AQI_summer	0.143	0.091	0.1205	0.120	0.1738	0.057
PRE	0.0107	0.989	0.0060	0.996	0.0237	0.950
SSD	0.0191	0.969	0.0150	0.979	0.0267	0.853
TEM	0.0107	0.989	0.0060	0.996	0.0237	0.950

Table 4. The qand p-values for each model. q represents the explanatory power of the risk factor. Normalized difference vegetation index (NDVI)_100m represents the NDVI level within a 100-m radius around the school. NDVI_5,000 m represents the NDVI level within a 5,000-m radius around the school. Sports area represents the number of sports area facilities within a 5,000-m radius around the school. AQI_winter represents the winter air quality index (AQI) within a 5,000-m radius around the school. AQI_summer represents the summer air quality index within a 5,000-m radius around the school. Precipitation rate (PRE) represents the annual average rainfall at the school location. Sunshine duration (SSD) represents the sunshine duration at the school location. Mean 2-meter temperature (TEM) represents the annual average temperature at the school location.

Risk factors	AGE	NDVI_100m	NDVI_5,000 m	Sports area	AQI_winter	AQI_summer	PRE	SSD
NDVI_100m	TE							
NDVI_5,000 m	TE	NA						
Sports area	TE	NA	NA					
AQI_winter	SNA	NA	NA	NA				
AQI_summer	TE	NA	NA	NA	NA			
PRE	TE	NA	NA	NA	NA	NA		
SSD	TE	NA	NA	NA	NA	NA	TE	
TEM	TE	NA	NA	NA	NA	NA	SNA	TE

Table 5. Interaction detection among the risk factors. Two-factor enhancement (TE) indicates that the combined effect of two factors is greater than that of a single factor. Nonlinear attenuation (NA) indicates that the combined effect of the two factors is greater than that of a single factor but less than the original effect. Single-factor non-linear attenuation (SNA) indicates that the combined effect of the two factors is less than that of either factor alone. Normalized difference vegetation index (NDVI)_100m represents the NDVI level within a 100-m radius around the school. NDVI_5,000 m represents the NDVI level within a 5,000-m radius around the school. Sports area represents the number of sports area facilities within a 5,000-m radius around the school. AQI_winter represents the winter air quality index (AQI) within a 5,000-m radius around the school. AQI_summer represents the summer air quality index within a 5,000-m radius around the school. Precipitation rate (PRE) represents the annual average rainfall at the school location. Sunshine duration (SSD) represents the sunshine duration at the school location. Mean 2-meter temperature (TEM) represents the annual average temperature at the school location.

Risk factors	AGE	NDVI_100m	NDVI_5,000 m	Sports area	AQI_winter	AQI_summer	PRE	SSD
NDVI_100m	Y							
NDVI_5,000 m	Y	Y						
Sports area	Y	Y	Y					
AQI_winter	Y	N	Y	Y				
AQI_summer	Y	N	Y	Y	N			
PRE	Y	Y	Y	Y	Y	Y		
SSD	Y	Y	Y	Y	Y	Y	Y	
TEM	Y	Y	Y	Y	Y	Y	N	Y

Table 6. Ecological detection among the risk factors. Y represents a significant difference in explaining school myopia ($p < 0.05$). N represents no significant difference ($p > 0.05$). Normalized difference vegetation index (NDVI)_100m represents the NDVI level within a 100-m radius around the school. NDVI_5,000 m represents the NDVI level within a 5,000-m radius around the school. Sports area represents the number of sports area facilities within a 5,000-m radius around the school. AQI_winter represents the winter air quality index (AQI) within a 5,000-m radius around the school. AQI_summer represents the summer air quality index within a 5,000-m radius around the school. Precipitation rate (PRE) represents the annual average rainfall at the school location. Sunshine duration (SSD) represents the sunshine duration at the school location. Mean 2-meter temperature (TEM) represents the annual average temperature at the school location.

Data availability

The datasets used and analyzed during the current study available from the corresponding author on reasonable request.

Received: 9 April 2024; Accepted: 25 November 2024
Published online: 02 December 2024

References

1. Dolgin, E. The myopia boom. *Nature* **519**(7543), 276–278 (2015).
2. Haarman, A. E. G. et al. The complications of myopia: a review and Meta-analysis. *Invest. Ophthalmol. Vis. Sci.* **61**(4), 49 (2020).
3. Jonas, J. B., Wang, Y. X., Dong, L. & Panda-Jonas, S. High myopia and Glaucoma-like Optic Neuropathy. *Asia Pac. J. Ophthalmol. (Phila)*. **9**(3), 234–238 (2020).
4. Ohno-Matsui, K. & Jonas, J. B. Posterior staphyloma in pathologic myopia. *Prog Retin Eye Res.* **70**, 99–109 (2019).
5. Bremond-Gignac, D. Myopie de l'enfant [Myopia in children]. *Med. Sci. (Paris)*. **36**(8–9), 763–768 (2020). French.
6. Morgan, I. G. et al. IMI Risk factors for myopia. *Invest. Ophthalmol. Vis. Sci.* **62**(5), 3 (2021).
7. Morgan, I. G. et al. The epidemics of myopia: Aetiology and prevention. *Prog Retin Eye Res.* **62**, 134–149 (2018).
8. Eppenberger, L. S. & Sturm, V. The role of Time exposed to Outdoor Light for Myopia Prevalence and Progression: A literature review. *Clin. Ophthalmol.* **14**, 1875–1890 (2020).
9. Ip, J. M. et al. Ethnic differences in refraction and ocular biometry in a population-based sample of 11-15-year-old Australian children. *Eye (Lond)*. **22**(5), 649–656 (2008).
10. Amanda, N. et al. Risk factors for Incident Myopia in Australian Schoolchildren. *Ophthalmology* **120**(10), 2100–2108 (2013).
11. French, A. N., Ashby, R. S., Morgan, I. G. & Rose, K. A. Time outdoors and the prevention of myopia. *Exp. Eye Res.* **114**, 58–68 (2013).
12. Yuan, T. & Zou, H. Effects of air pollution on myopia: An update on clinical evidence and biological mechanisms. *Environ. Sci. Pollut Res. Int.* **29**(47), 70674–70685 (2022).
13. Yang, Y. et al. Spatial technology assessment of green space exposure and myopia. *Ophthalmology* **129**(1), 113–117 (2022).
14. Lu, C. et al. Socioeconomic disparities and green space associated with myopia among Chinese school-aged students: A population-based cohort study. *J. Glob Health*. **14**, 04140 (2024).
15. Yang, Y. et al. Green space morphology and school myopia in China. *JAMA Ophthalmol.* **142**(2), 115–122 (2024).
16. Klompmaker, J. O. et al. Green space definition affects associations of green space with overweight and physical activity. *Environ. Res.* **160**, 531–540 (2018). Epub 2017 Oct 26. PMID: 29106952.
17. Medina, A. The cause of myopia development and progression: Theory, evidence, and treatment. *Surv. Ophthalmol.* **67**(2), 488–509 (2022). Epub 2021 Jun 25. PMID: 34181975.
18. Medina, A. Models of myopia: The effect of accommodation, lenses and atropine. *Eye (Lond)*. **38**(7), 1290–1295 (2024). Epub 2023 Dec 12. PMID: 38087120; PMCID: PMC11076616.
19. Ruan, Z. et al. Ambient fine particulate matter and ozone higher than certain thresholds associated with myopia in the elderly aged 50 years and above. *Environ. Res.* **177**, 108581 (2019).
20. Chen, X. et al. Prevalence, incidence, and risk factors for myopia among urban and rural children in southern China: Protocol for a school-based cohort study. *BMJ Open*. **11**(11), e049846 (2021).
21. Johannessen, A., Xu, S., Abbah, A. P. & Janson, C. Greenness exposure: Beneficial but multidimensional. *Breathe (Sheff)*. **19**(2), 220221 (2023).
22. Zhang, C. et al. Effects of greenness on myopia risk and school-level myopia prevalence among high school-aged adolescents: Cross-sectional study. *JMIR Public. Health Surveil* **9**, e42694. (2023).
23. Bao, W. W. et al. Urban greenspace and visual acuity in schoolchildren: A large prospective cohort study in China. *Environ. Int.* **184**, 108423 (2024).
24. National, M. *Daily Meteorological Dataset of Basic Meteorological Elements of China National Surface Weather Station (V3.0)(1951–2010)* (National Tibetan Plateau / Third Pole Environment Data Center, 2019).
25. Song, Y., Wang, J., Ge, Y. & Xu, C. An optimal parameters-based geographical detector model enhances geographic characteristics of explanatory variables for spatial heterogeneity analysis: Cases with different types of spatial data. *GIScience Remote Sens.* **57**(5), 593–610 (2020).

26. R Core Team. R: A language and environment for statistical computing. R Foundation for Statistical Computing, Vienna, Austria. (2023). https://www.R-project.org/
27. French, A. N., Morgan, I. G., Burlutsky, G., Mitchell, P. & Rose, K. A. Prevalence and 5- to 6-year incidence and progression of myopia and hyperopia in Australian schoolchildren. *Ophthalmology* **120**(7), 1482–1491 (2013).
28. Ferraz, F. H., Corrente, J. E., Opromolla, P., Padovani, C. R. & Schellini, S. A. Refractive errors in a Brazilian population: Age and sex distribution. *Ophthalmic Physiol. Opt.* **35**(1), 19–27 (2015).
29. Li, D. L. et al. Lower indoor spatial frequency increases the risk of myopia in children. *Br. J. Ophthalmol.* Aug 8:bjo-2024-325888 (2024). Epub ahead of print. PMID: 39122351.
30. Flitcroft, D. I., Harb, E. N. & Wildsoet, C. F. The spatial frequency content of urban and indoor environments as a potential risk factor for Myopia Development. *Invest. Ophthalmol. Vis. Sci.* **61**(11), 42 (2020). PMID: 32986814; PMCID: PMC7533745.
31. Wu, P. C. et al. Myopia prevention and outdoor light intensity in a school-based cluster randomized trial. *Ophthalmology* **125**(8), 1239–1250 (2018).
32. Manferdelli, G., La Torre, A. & Codella, R. Outdoor physical activity bears multiple benefits to health and society. *J. Sports Med. Phys. Fit.* **59**(5), 868–879 (2019).
33. Mu, J. et al. Research trends and hotspots in the relationship between outdoor activities and myopia: A bibliometric analysis based on the web of science database from 2006 to 2021. *Front. Public. Health*. **10**, 1047116 (2022).
34. Karthikeyan, S. K., Ashwini, D. L., Priyanka, M., Nayak, A. & Biswas, S. Physical activity, time spent outdoors, and near work in relation to myopia prevalence, incidence, and progression: An overview of systematic reviews and meta-analyses. *Indian J. Ophthalmol.* **70**(3), 728–739 (2022).
35. Ashby, R., Ohlendorf, A. & Schaeffel, F. The effect of ambient illuminance on the development of deprivation myopia in chicks. *Invest. Ophthalmol. Vis. Sci.* **50**(11), 5348–5354 (2009). Epub 2009 Jun 10. PMID: 19516016.
36. Herbort, C. P., Papadia, M. & Neri, P. Myopia and inflammation. *J. Ophthalmic Vis. Res.* **6**(4), 270–283 (2011).
37. Jung, S. J., Mehta, J. S. & Tong, L. Effects of environment pollution on the ocular surface. *Ocul Surf.* **16**(2), 198–205 (2018).
38. Xu, R., Zheng, J., Liu, L. & Zhang, W. Effects of inflammation on myopia: Evidence and potential mechanisms. *Front. Immunol.* **14**, 1260592 (2023). PMID: 37849748; PMCID: PMC10577208.
39. Zhu, X. et al. Association between TGF-β gene polymorphism and myopia: A systematic review and meta-analysis. *Med. (Baltim).* **101**(30), e29961. (2022). PMID: 35905284; PMCID: PMC9333477.
40. Diener, A. & Mudu, P. How can vegetation protect us from air pollution? A critical review on green spaces' mitigation abilities for air-borne particles from a public health perspective - with implications for urban planning. *Sci. Total Environ.* **796**, 148605 (2021). Epub 2021 Jun 24. PMID: 34271387.
41. Ma, Y. et al. Myopia screening: Combining visual acuity and noncycloplegic autorefraction. *Optom. Vis. Sci.* **90**(12), 1479–1485 (2013).
42. Ozdemir, O., Özen Tunay, Z., Petriçli, I. S., Ergintürk Acar, D. & Erol, M. K. Comparison of non-cycloplegic photorefraction, cycloplegic photorefraction and cycloplegic retinoscopy in children. *Int. J. Ophthalmol.* **8**(1), 128–131 (2015).
43. Kang, M. T. et al. Prevalence and risk factors of pseudomyopia in a Chinese children population: The Anyang Childhood Eye Study. *Br. J. Ophthalmol.* **105**(9), 1216–1221 (2021).
44. Sun, W. et al. Pseudomyopia as an independent risk factor for myopia onset: A prospective cohort study among school-aged children. *Br. J. Ophthalmol.* **108**(6), 873–878 (2024).
45. Du, R. & Ohno-Matsui, K. Novel uses and challenges of artificial intelligence in diagnosing and managing eyes with high myopia and pathologic myopia. *Diagnostics (Basel).* **12**(5), 1210 (2022). Published 2022 May 12.

Acknowledgements
Supported by National Natural Science Foundation of China (NO. 42201457) and National Natural Science Foundation of China (NO. 42301486).

Author contributions
Qi Cui, Yishuang Xu and Fan Li contributed equally to this work.All authors reviewed the manuscript.

Funding information
National Natural Science Foundation of China (NO. 42201457); National Natural Science Foundation of China (NO.42301486).

Declarations

Competing interests
The authors declare no competing interests.

Additional information
Correspondence and requests for materials should be addressed to Z.C., X.H. or D.H.